NASA TM-81189

NASA Technical Memorandum 81169

AVRADCOM Technical Report 80-A-4

Comparison of Calculated and Measured Model Rotor Loading and Wake Geometry

Wayne Johnson

April 1980

National Aeronautics and Space Administration

United States Army Aviation Research and Development Command

NASA Technical Memorandum 81189

AVRADCOM Technical Report 80-A-4

Comparison of Calculated and Measured Model Rotor Loading and Wake Geometry

Wayne Johnson, Aeromechanics Laboratory
AVRADCOM Research and Technology Laboratories
Ames Research Center, Moffett Field, California

NASA
National Aeronautics and Space Administration
Ames Research Center
Moffett Field, California 94035

United States Army
Aviation Research and Development Command
St. Louis, Missouri 63166

COMPARISON OF CALCULATED AND MEASURED MODEL ROTOR LOADING AND WAKE GEOMETRY

Wayne Johnson*

Ames Research Center

and

Aeromechanics Laboratory

AVRADCOM Research and Technology Laboratories

ABSTRACT

Calculated blade bound circulation and wake geometry are compared with measured results for a model helicopter rotor in hover and forward flight. Hover results are presented for rectangular tip and ogee tip planform blades. The correlation is quite good when the measured wake geometry characteristics are used in the analysis. Available prescribed wake geometry models are found to give fair predictions of the loading, but they do not produce a reasonable prediction of the induced power. Forward flight results are presented for twisted and untwisted blades. Fair correlation between measurements and calculations is found for the bound circulation distribution on the advancing side. The tip vortex geometry in the vicinity of the advancing blade in forward flight was predicted well by the free wake calculation used, although the wake geometry did not have a significant influence on the calculated loading and performance for the cases considered.

---

*Head of Rotorcraft Research Section, Large-Scale Aerodynamics Branch

INTRODUCTION

A series of experiments have been conducted at Ames Research Center, in which a laser velocimeter was employed to measure the flow field of a model helicopter rotor. The results of these experiments have included measured bound circulation and tip vortex location for a hovering rotor with two blade tip planforms;[1,2] measured bound circulation on the advancing side of the rotor in forward flight;[3] and measured tip vortex position on the advancing side in forward flight, for two blade twist values.[4,5] Each of these experiments used a two-bladed rotor with a radius of approximately 1 meter, operated at low tip speed. The forward flight experiments were conducted in a 7- by 10-ft wind tunnel. A two-component laser velocimeter was used to measure the flow field in the rotor wake. The blade loading was obtained by measuring the circulation around a box enclosing the blade at a specified radial station. The wake geometry, in terms of the location of the tip vortices, was obtained from measurements of the induced velocity along radial and vertical traverses through the wake. Complete details of the experiments are given in the original papers.[1-5]

A principal objective of this series of experiments has been to provide data for the development and verification of rotor analytical models. The purpose of the present paper is to compare the measured loading and wake geometry with calculated results. For the calculations, a recently developed helicopter analysis was used.[6] The rotor wake analysis was based on a discrete element representation of the vorticity, with models for the wake rollup and the distorted wake geometry. The loading was calculated using lifting line theory, with corrections available for three-dimensional

effects at the tip and at vortex/blade interactions. The rotor blade flapping motion was calculated by means of a harmonic analysis method. An existing analysis was used to calculate the distorted, free wake geometry in forward flight.[7]

ANALYTICAL MODEL

A top view of the wake model is shown in figure 1. The induced velocity, circulation, and lift are evaluated at 15 stations along the blade, as shown by the dots. The trailed vorticity in the wake directly behind the blade is represented by discrete vortex lines positioned midway between the points at which the circulation is calculated. The strength of each trailed line is defined by the difference between the bound circulation at successive radial stations. This part of the model is a common numerical implementation of lifting line theory. For the rotary wing it is necessary also to model the rollup of the vorticity into a concentrated tip vortex, because the blade encounters the wake from the preceding blades as it rotates. Therefore, after an azimuthal extent of 30° in this case, the trailed vorticity is concentrated into a single tip vortex line, with strength equal to the maximum bound circulation of the blade. The azimuthal extent of the near wake was varied from 15° to 60° (and the number of radial stations from 10 to 15) with little effect on the calculated loading. The key element in the model is the vorticity distribution in the wake when it encounters the following blade, at which point it must be concentrated into the tip vortex. For conservation of vorticity, there must be an inboard sheet of trailed vorticity with equal total strength and opposite sign as the tip vortex. This inboard sheet is much less important

than the tip vortex, partly because the vorticity is not as concentrated and partly because it is convected downward at about twice the rate as the tip vortex.[8] Consequently the entire inboard sheet can be reasonably represented as a single vortex line, shown dashed in figure 1, with a large core radius (43% of the rotor radius in this case) to avoid unrealistically large induced velocities when the wake passes under the following blade. A similar wake model is used for the other blade of the rotor. The detailed near wake model need not be used for the second blade since it is far from where the induced velocity is being calculated on the first blade (figure 1). The curved trailed vortex elements in the wake are represented by a connected series of straight line segments, with an azimuthal increment of 15° in this case. Five revolutions of the wake behind each blade are modelled in this fashion (only the first one-half revolution is shown in figure 1). An additional 30 revolutions of the wake are modelled using rectangular vortex sheet panels to construct a cylinder of axial and circumferential vorticity representing the tip vortices, and an axial line vortex representing the root vortices. By this means the wake far from the rotor blade (extending approximately from 2 to 10 rotor radii below the disk) is economically accounted for; if this part of the wake were neglected, the induced velocity at the rotor disk would be significantly underestimated.

The geometry of the tip vortex in hover is described by the following coordinates:

$$x = (1 + D_r) \cos(\Psi - \phi)$$
$$y = (1 + D_r) \sin(\Psi - \phi)$$
$$z = D_z$$

A tip-path plane coordinate system with origin centered on the rotor shaft is used; x and y are rectangular coordinates in the rotor plane; z is measured vertically upward from the plane of the blade tips. The azimuth angle of the rotor blade is Ψ, measured from the x axis; ϕ is the wake age, i.e. the azimuth angle along the wake helix, measured from the rotor blade. D_z and D_r are the vertical and radial distortions of the wake due to its self-induced velocity. A two-stage vertical convection and exponential radial contraction model is used for hover:[8]

$$D_z = \begin{cases} -K_1 \phi & \phi < \pi \\ -K_1 \pi \quad -K_2(\phi - \pi) & \phi > \pi \end{cases}$$

$$D_r = -(1 - e^{-K_3 \phi})(1 - K_4)$$

(a similar model is used for the distortion of the inside and outside edges of the inboard wake sheet, but only the tip vortex geometry has a significant effect on the loading). The parameters K_1, K_3, and K_4 determine the position of the tip vortex when it encounters the following blade; K_4 determines the contracted radius in the far wake; and K_2 determines the vertical convection after the first blade passage. An undistorted wake geometry can be obtained using $D_r = 0$ and $D_z = -\phi \bar{\lambda}$, where $\bar{\lambda}$ is the mean inflow ratio at the rotor disk.

A similar wake model is used for the forward flight calculations. The bound circulation in forward flight varies azimuthally as well as radially, so the shed wake is also included. The shed wake is modelled by radial, discrete vortex lines. The vorticity strength varies linearly along each vortex line element, both trailed and shed. In forward flight it is only necessary to use two revolutions of the wake behind each blade

to calculate the induced velocity. The geometry of the tip vortex relative to the tip-path plane is described by the following coordinates:

$$x_{tpp} = \cos(\Psi - \phi) + \phi/\mu + D_x(\Psi, \phi)$$

$$y_{tpp} = \sin(\Psi - \phi) + D_y(\Psi, \phi)$$

$$z_{tpp} = \phi/\mu \tan\alpha_{tpp} + D_z(\Psi, \phi)$$

where μ is the rotor advance ratio (forward speed divided by tip speed) and α_{tpp} is the angle of attack of the tip-path plane, positive for rearward tilt. The coordinate x_{tpp} is positive downstream, and y_{tpp} is positive to the right. Wind or tunnel axis coordinates are obtained by accounting for the blade flapping motion:

$$z = z_{tpp} + \beta_p + (\beta_{1c} - \alpha_s)x + \beta_{1s} y$$

where β_p is the blade precone angle, β_{1c} and β_{1s} are the longitudinal and lateral flapping angles (relative to the shaft), and α_s is the shaft angle of attack. An undistorted wake geometry, that only accounts for the vertical convection due to the mean induced velocity, is obtained using $D_x = D_y = 0$ and $D_z = -\phi\lambda$. A free wake geometry calculation can also be used.

HOVER RESULTS

Experimental data are available for the circulation and wake geometry in hover with two tip shapes, rectangular and ogee.[1,2] The principal parameters defining the rotor and operating conditions are given in Table 1; further details, particularly for the twist distribution and ogee tip planform are given in the original papers. The ogee tip planform extends over the outer 10% span of the blade. The solidity used for the ogee tip is the thrust-equivalent values (radius-squared weighted). In all calculations,

Table 1. Rotor parameters and operating condition for hover cases.

	Rectangular Tip Blades	Ogee Tip Blades
Blade radius, R	1.045 m	1.045 m
Rotor tip speed	76.6 m/sec	76.6 m/sec
Number of blades	2	2
Chord, c/R	0.0729	0.0729
Precone	1.5°	1.5°
Twist	-11°	-11°
Solidity, σ	0.0464	0.0396
Thrust, C_T/σ	0.099	0.103

the rotor thrust was trimmed to the value given in Table 1, which was obtained by integrating the measured loading distribution.

The calculated and measured circulation distributions are compared in figure 2 for the rectangular tip blade in hover. The calculations used the measured position of the tip vortex when it first passed under the following blade, and a value of $K_2 = 0.0550$. A tip loss factor of $B = 0.985$ was used. The correlation exhibited in figure 2 is quite good. The wake geometry used is shown in figure 3, in terms of the intersections of the tip vortices with a vertical plane under the rotor blade (the x-y plane, with the blade at azimuth angle $\Psi = 90^{\circ}$). The undistorted wake geometry is also shown in figure 3, and figure 4 shows the corresponding calculated circulation. Without a proper modelling of the wake contraction, the calculated loading distribution is very different from the measured distribution.

Prescribed wake geometry models for hovering rotors have been developed by Landgrebe[9] and by Kocurek and Tangler.[10] They developed empirical expressions for the constants K_1, K_2, K_3, and K_4 by matching rotor wake geometry data obtained using flow visualization techniques. Figures 5 and 6 show the loading calculated using these two wake geometry models. For the present case, the only significant difference between the Landgrebe model and the Kocurek and Tangler model is in the parameter K_1, hence in the vertical separation of the vortex when it first encounters the following blade (see figure 3). The Landgrebe model places the vortex a small distance (1.1% R) closer to the blade, hence the peak bound circulation is somewhat larger than for the Kocurek and Tangler model (compare figures

5 and 6). These prescribed wake models give a value of $K_2 = 0.0608$. Figure 7 shows the loading calculated using the measured location for the tip vortex when it first passes under the blade, and a value of $K_2 = 0.0608$. Figures 5, 6, and 7 differ only in the location of the first vortex under the blade. The data used to construct the prescribed wake models,[9,10] show a scatter in the vortex position of perhaps ± 1 to 2% of the blade radius. Within that accuracy, the tip vortex geometries defined by the two models are identical for this case, and both correctly predict the location of the first vortex under the blade. However, although the differences in the vortex positions are slight, using the measured position (figure 7) definitely improved the calculated loading distribution, compared with using the prescribed wake models (figures 5 and 6).

Figures 2 and 7 differ only in the value of the parameter K_2, which is the vertical convection rate after the vortex first encounters the following blade. The measured wake geometry data does not provide a value for K_2. Initially therefore the loading was calculated using the same value of K_2 as given by the prescribed wake models (figure 7). By using a 10% smaller value of K_2, the correlation of the measured and calculated circulation distributions was definitely improved (figure 2). The calculated performance provides further support for the use of a smaller value of K_2 than obtained from the prescribed wake models. Using $K_2 = 0.0608$ (figure 7), the calculated induced power was only 3% higher than the ideal momentum-theory induced loss, which is much better performance than would be expected, especially with two blades. Using $K_2 = 0.0550$ (figure 2), the calculated induced power was 12% higher than ideal, a more reasonable value.

The calculated and measured circulation distributions are compared in figure 8 for the ogee tip blade in hover. The calculations used the measured position of the tip vortex when it first passed under the following blade, and a value of $K_2 = 0.0500$ (figure 3). With the ogee planform, the measured data show the tip vortex rollup occurring at a radial station of 94% R. It was possible to properly model this rollup position in the analysis by simply using a tip loss factor of $B = 0.94$. The correlation exhibited in figure 8 is nearly as good as for the rectangular tip blade. For the ogee tip there are no corresponding prescribed wake models to provide a guide for the choice of K_2; the wake convection must be specified on the basis of the peak circulation and the predicted induced power. Properly modelling the tip vortex rollup at 94% R is essential for an accurate calculation of the loading distribution. For comparison, figure 9 shows the loading calculated for the ogee tip when the vortex rollup remains at $r/R = 1$, as for the rectangular blade. It is interesting to note that the ogee tip blade can be considered equivalent to a rectangular tip blade with a radius of 94% R as regards the bound circulation distribution and wake geometry;[1] and as regards the rotor performance parameters (disk loading, induced power, and figure of merit). Of course, the ogee planform in addition produces a tip vortex with a larger core radius and smaller peak velocity.

FORWARD FLIGHT RESULTS

Experimental data are available for the circulation and wake geometry in forward flight for blades with zero twist and -11° twist.[3-5] The principal parameters defining the rotor and operating conditions are given in Table 2. The measured bound circulation is available only for the

Table 2. Rotor parameters and operating condition for forward flight cases.

	Zero Twist Blades	-11° Twist Blades
Blade radius, R	1.066 m	1.045 m
Rotor tip speed	67.0 m/sec	65.7 m/sec
Number of blades	2	2
Chord, c/R	0.1012	0.0729
Precone	1.5°	1.5°
Solidity, σ	0.0644	0.0464
Lock number, γ	3.3	3.78
Advance ratio, $V/\Omega R$	0.18	0.18
Shaft angle, α_s	-10°	-10°
Collective pitch, Θ_{75}	8.5°	10.1°
Tip-path plane angle, α_{tpp}	-6.6°	-5.5°

untwisted blade, on the advancing side at $\psi = 90^\circ$. The measured and calculated circulation distributions are compared in figure 10. The circulation box encloses some of the shed wake vorticity, which is equivalent to measuring the circulation of the blade when it is at a slightly earlier azimuth position; hence the calculated loading at $\psi = 75^\circ$ is also shown. The correlation exhibited in figure 10 is fair, although both the scatter in the measured data and the differences between the measured and calculated results are larger than for the hover cases. The calculated loading in figure 10 was obtained using the free wake geometry model, but the results obtained using an undistorted wake geometry were nearly the same. Using the two wake models, only small differences were produced in the calculated thrust, power, and flapping. However, using nonuniform wake-induced velocity produced large differences compared with using uniform inflow (with uniform induced velocity, the bound circulation at $\psi = 90^\circ$ would be a linear function of the radial station r/R).

Measurements are available for the geometry of the tip vortex from the blade at $\psi = 270^\circ$, in the vicinity of the other blade at $\psi = 90^\circ$ on the advancing side.[5] Figures 11 and 12 compare the calculated free wake geometry results with the measured tip vortex position for the untwisted blades. A top view is shown in figure 11 and a side view in figure 12. A tunnel or wind axis system is used, with the x coordinate directed downstream, the y coordinate toward the advancing side, and the z coordinate upward. The rotor hub is the center of the coordinate system. The wake geometry is calculated at 15° azimuth intervals, so the range of the experimental data is covered by just two vortex line segments. The corresponding results

for the -11° twist blades are shown in figures 13 and 14. Figures 12 and 14 also show the geometry obtained using the undistorted wake model. The correlation between the measured and calculated free wake geometry is good, considering that the calculation does not attempt to model the fine details of the geometry. At this point in the wake, the predicted distortion is small in the x and y directions. The vertical convection is significant however, and has the net effect of keeping the vortex in the vicinity of the blade at $\Psi = 90^{\circ}$ nearly parallel to the tip-path plane (which is tilted forward relative to the tunnel axes). This trend is confirmed by the measured positions. In contrast, the undistorted geometry shows the tip vortex being steadily convected downward relative to the tip-path plane as the element age increases.

It must be recognized however that the experimental data does not provide a particularly severe test of the free wake calculation. The tip-path plane angle of attack is fairly large, and the tip vortex encounters the following blade with substantial vertical separation. Consequently the tasks of calculating the wake geometry and loading are easier than for small tip-path plane angle of attack. In fact, although the use of nonuniform inflow is important, there is little difference for this case between the free wake results and the undistorted wake results, as regards the performance and blade loading.

CONCLUSIONS AND RECOMMENDATIONS

Calculated blade bound circulation and wake geometry have been compared with measured results for a model helicopter rotor in hover and

forward flight. Quite good correlation was found for the predicted and measured circulation distributions in hover. This correlation was only possible using the measured wake geometry characteristics, including the tip vortex rollup, the radial and vertical position of the vortex when it first encounters the following blade, and the vertical convection rate in the far wake. An accurate wake geometry calculation will be necessary for a completely analytical calculation of hover performance and loading. The wake geometry defined by the available prescribed wake models was found to give the general features of the loading distribution well, although significant changes in the peak loading are produced by geometry differences that are within the scatter of the data from which the prescribed wake models were constructed. Moreover, a reasonable prediction of the induced power (which is very sensitive to the wake geometry changes) was not obtained using the prescribed wake models. The correlation between the calculated and measured circulation distributions in forward flight was acceptable, but not as good as for the hover cases. The tip vortex geometry in the vicinity of the advancing blade in forward flight was predicted fairly well by the free wake calculation used, although for these cases the wake geometry did not have a significant influence on the calculated loading and performance.

The experimental program that produced the data examined in this paper is continuing. The work in hover will be expanded to include variations in the number of blades, thrust, planform, and tip Mach number. It should be possible in these tests to also measure the vertical convection rate after the tip vortex first encounters the following blade. In future forward flight tests, it will be possible to measure the loading at azimuthal stations on

the front and rear of the disk, by using a three-component laser velocimeter system. It is recommended that data be obtained at only a few azimuth stations, for a wide range of rotor operating conditions (as opposed to collecting data at enough azimuth stations to define the loading distribution over the entire disk, but only for one or two operating conditions). Even more useful would be the loading at a fixed radial station as a function of azimuth, since vortex-induced loads are more readily discerned when the loading is viewed as a function of azimuth rather than radius. The operating conditions should include cases of small tip-path plane incidence, to provide a better test of the loading and wake geometry predictions.

REFERENCES

1. Ballard, John D.; Orloff, Kenneth L.; and Luebs, Alan B., "Effect of Tip Shape on Blade Loading Characteristics for a Two-Bladed Rotor in Hover," 35th Annual National Forum of the American Helicopter Society, Washington, D.C., May 1979
2. Ballard, John D.; Orloff, Kenneth L.; and Luebs, Alan B., "Effect of Tip Planform on Blade Loading Characteristics for a Two-Bladed Rotor in Hover," NASA TM-78615, November 1979
3. Biggers, James C.; Chu, Sing; and Orloff, Kenneth L., "Laser Velocimeter Measurements of Rotor Blade Loads and Tip Vortex Rollup," 31st Annual National Forum of the American Helicopter Society, Washington, D.C., May 1975
4. Biggers, James C.; Lee, Albert; Orloff, Kenneth L., and Lemmer, Opal J., "Measurements of Helicopter Rotor Tip Vortices," 33rd Annual National Forum of the American Helicopter Society, Washington, D.C., May 1977
5. Biggers, James C.; Lee, Albert; Orloff, Kenneth L.; and Lemmer, Opal J., Laser Velocimeter Investigation of Helicopter Rotor Tip Vortices," NASA TM X-73238, March 1977
6. Johnson, Wayne, "A Comprehensive Analytical Model of Rotorcraft Aerodynamics and Dynamics," NASA TM-81182, 1980
7. Scully, M.P., "Computation of Helicopter Rotor Wake Geometry and its Influence on Rotor Harmonic Airloads," Massachusetts Institute of Technology, ASRL TR 178-1, March 1975

8. Gray, Robin B., "On the Motion of the Helical Vortex Shed from a Single-Bladed Hovering Model Helicopter Rotor and its Application to the Calculation of the Spanwise Aerodynamic Loading," Princeton University, Aeronautical Engineering Department, Report No. 313, September 1955

9. Landgrebe, Anton J., "The Wake Geometry of a Hovering Helicopter Rotor and its Influence on Rotor Performance," Journal of the American Helicopter Society, Volume 17, Number 4, October 1972

10. Kocurek, J. David, and Tangler, James L., "A Prescribed Wake Lifting Surface Hover Performance Analysis," Journal of the American Helicopter Society, Volume 22, Number 1, January 1977

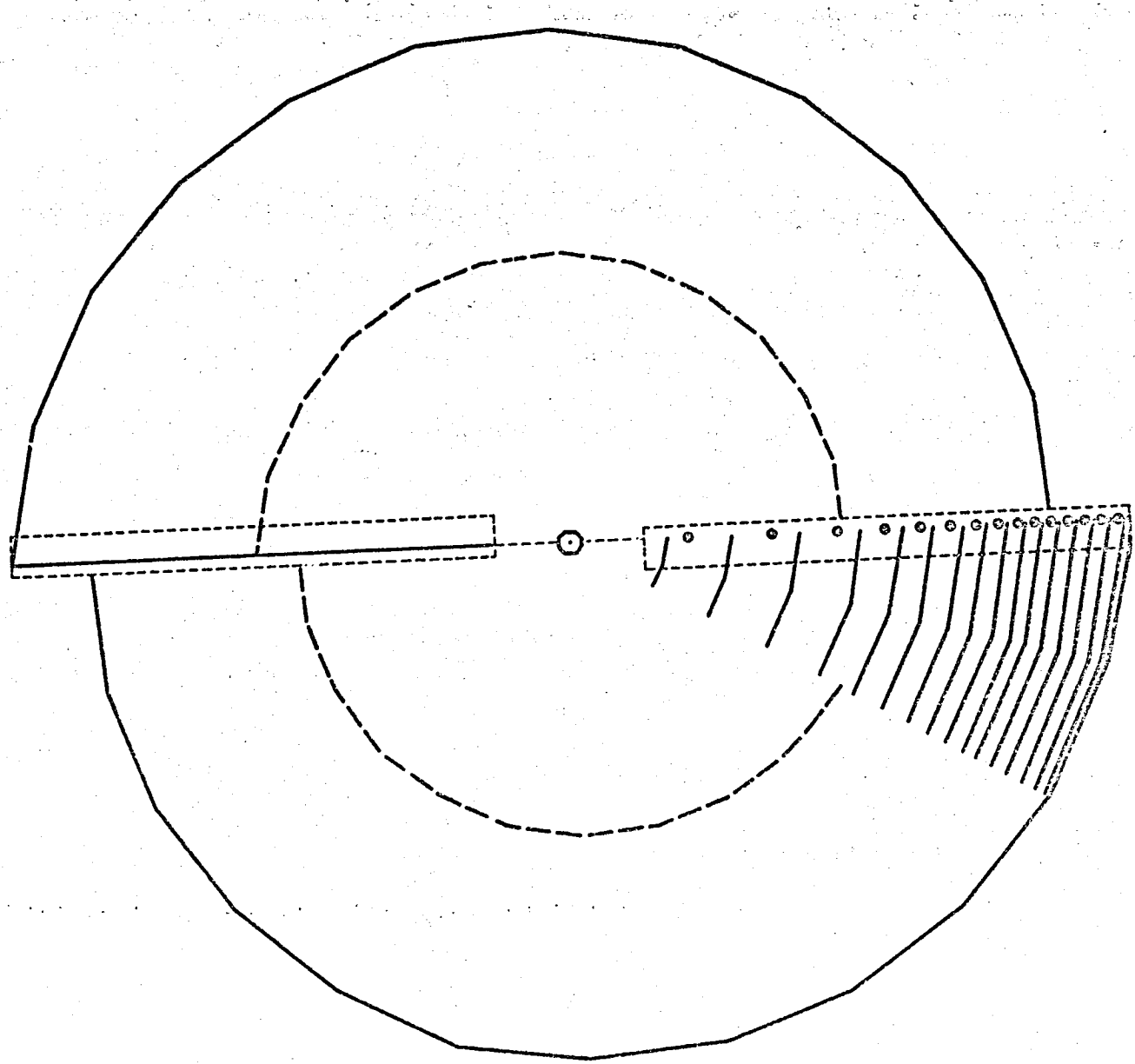

Figure 1. Sketch of wake model in hover (top view)

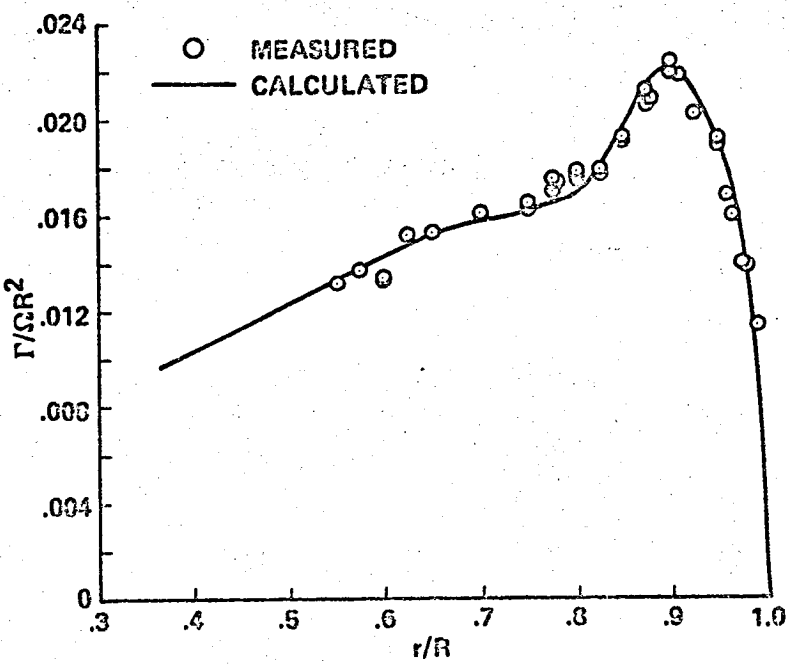

Figure 2. Comparison of measured and calculated circulation for rectangular tip blade in hover, with measured wake geometry and $K_2 = 0.0550$

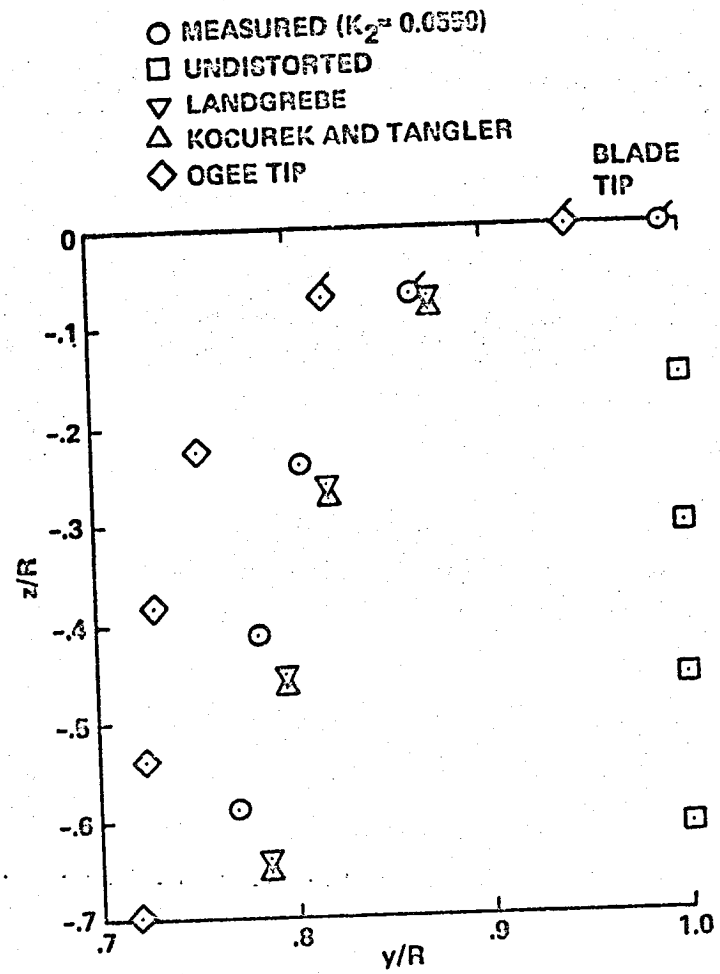

Figure 3. Location of tip vortices in hover (intersections with vertical plane under rotor blade; flagged points obtained by LV measurements)

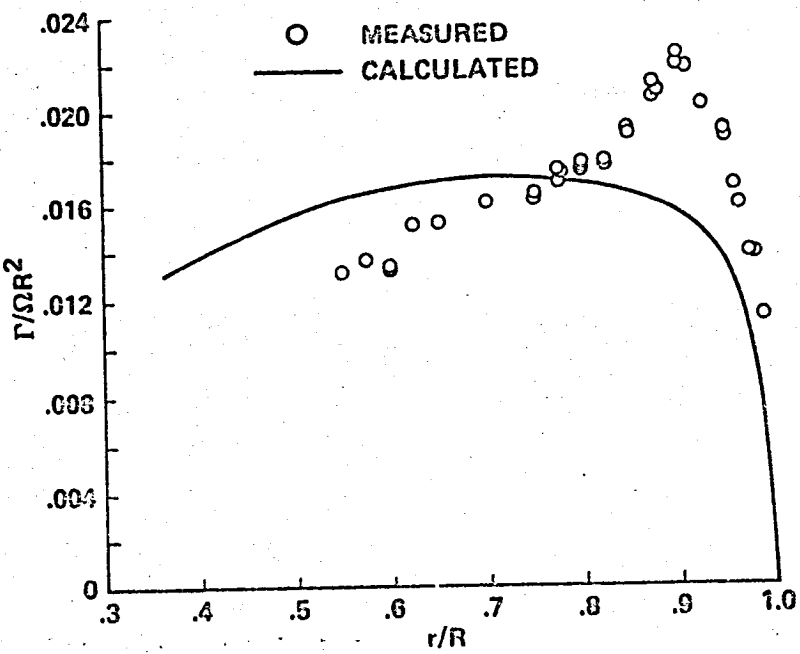

Figure 4. Bound circulation calculated with undistorted wake geometry

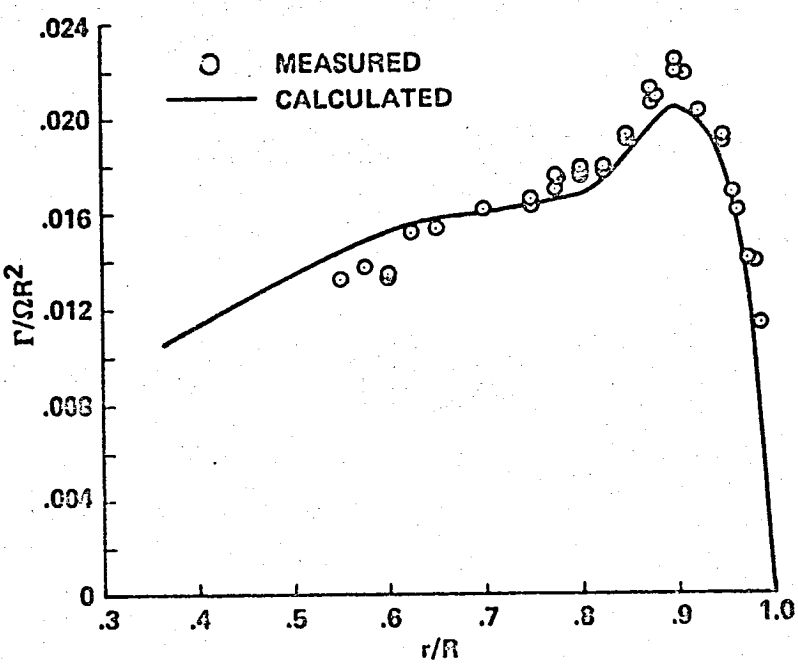

Figure 5. Bound circulation calculated with Landgrebe wake geometry

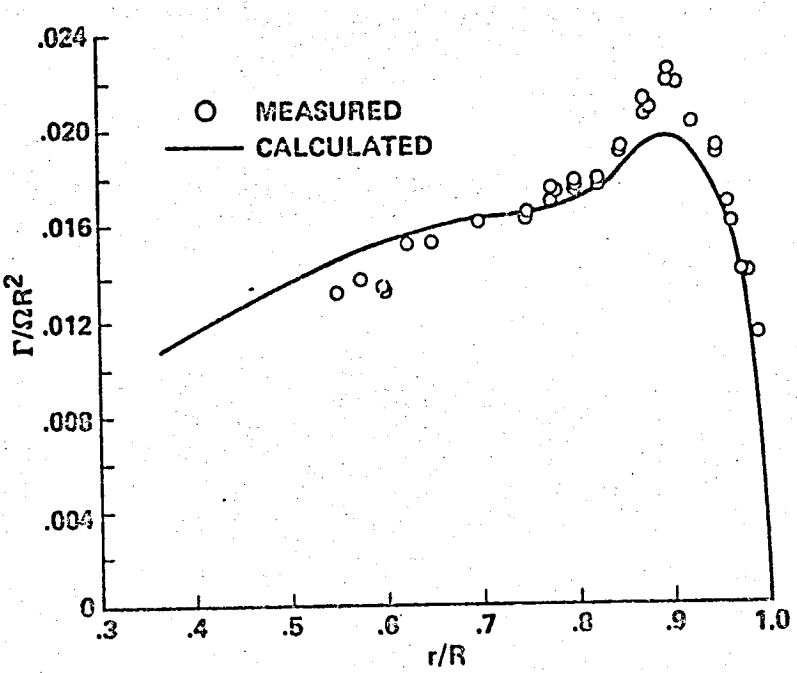

Figure 6. Bound circulation calculated with Kocurek and Tangler wake Geometry

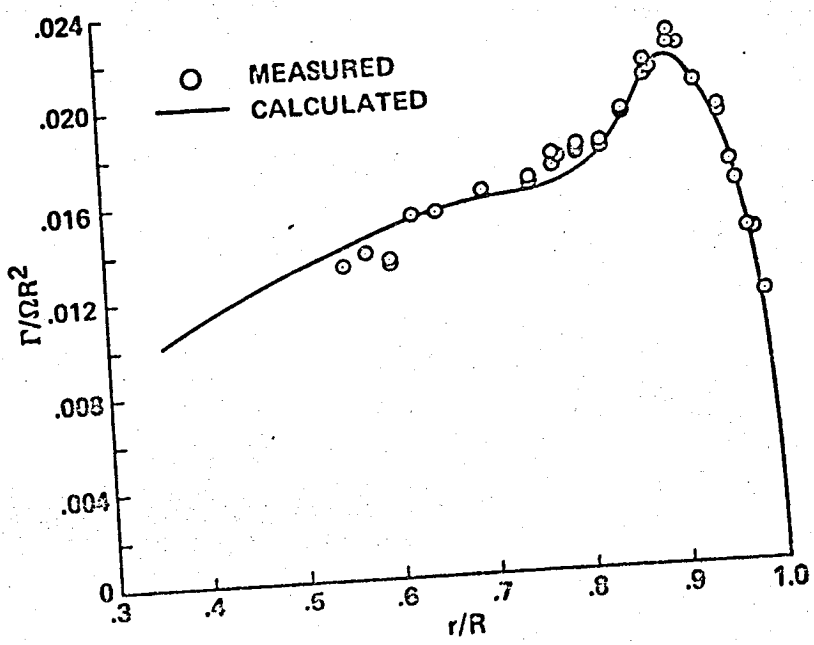

Figure 7. Bound circulation calculated with measured wake geometry and $K_2 = 0.0608$

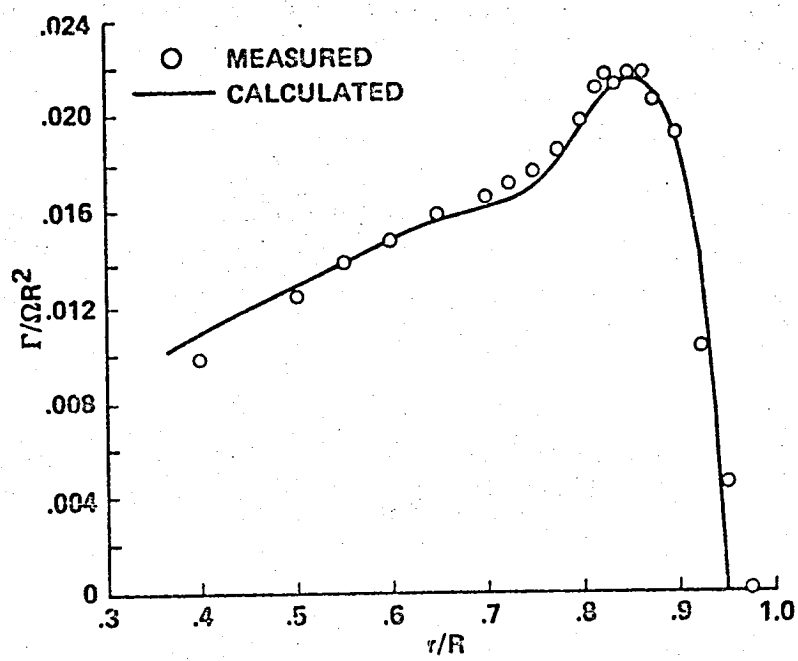

Figure 8. Comparison of measured and calculated circulation for ogee tip blade in hover

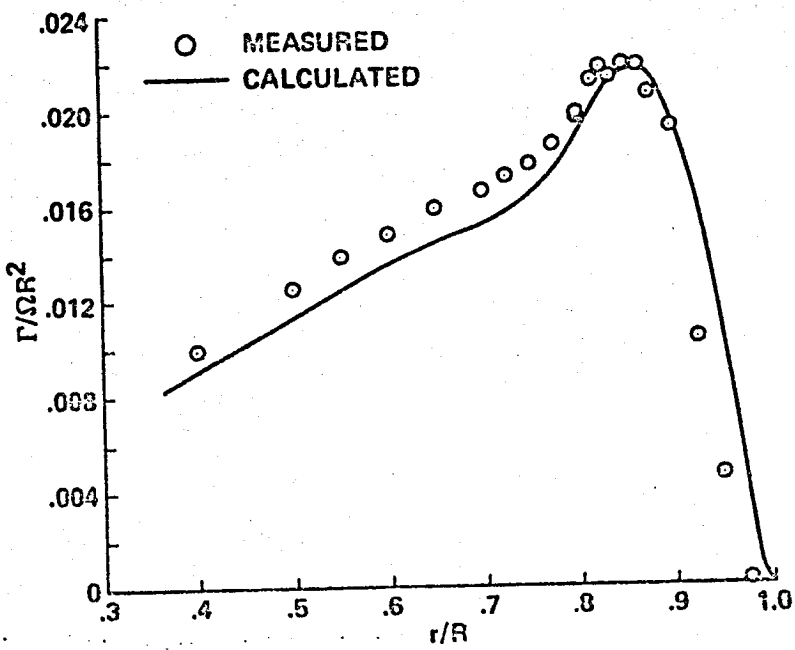

Figure 9. Bound circulation calculated for ogee tip blade with tip vortex rollup at r/R = 1.

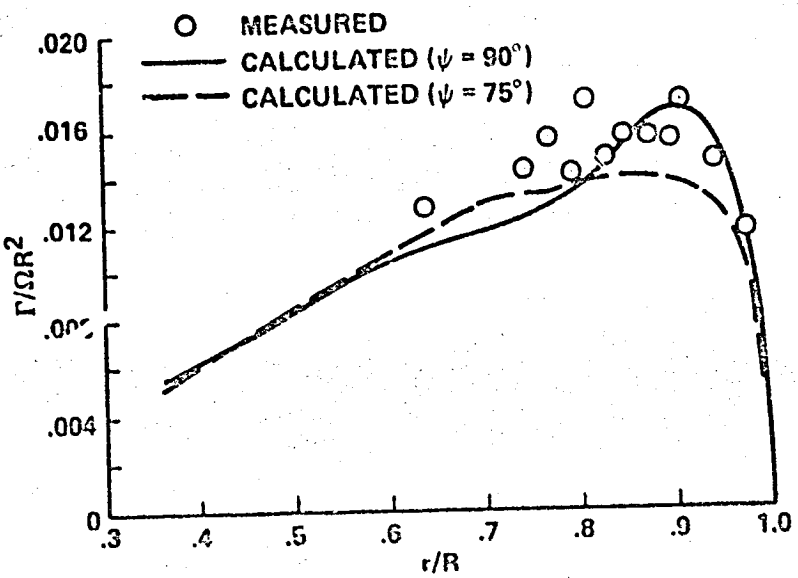

Figure 10. Comparison of measured and calculated circulation on the advancing side in forward flight ($V/\Omega R = 0.18$, untwisted blade)

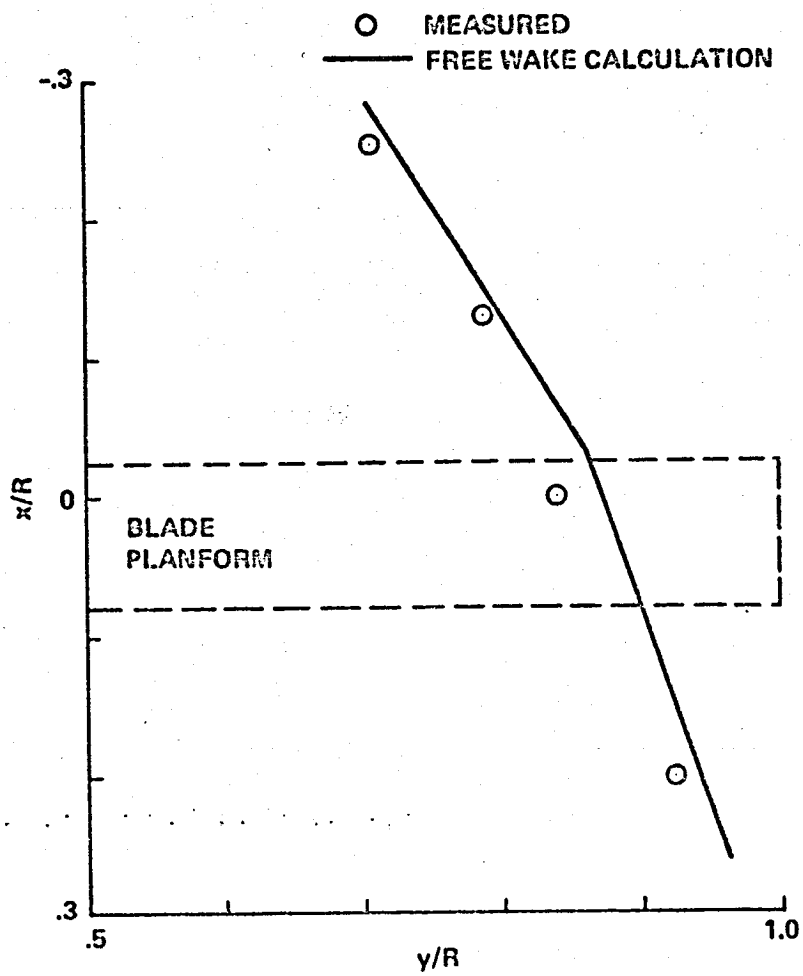

Figure 11. Top view of tip vortex geometry in vicinity of blade at $\Psi = 90^{\circ}$ ($V/\Omega R = 0.18$, untwisted blade)

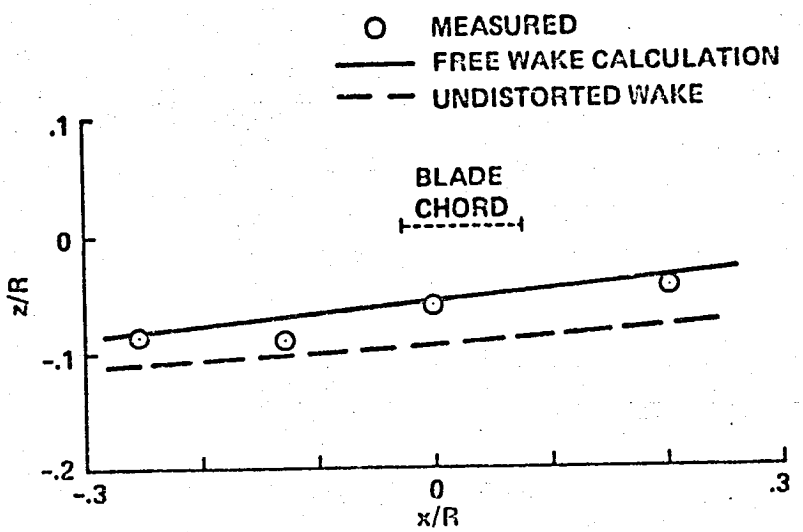

Figure 12. Side view of tip vortex geometry in vicinity of blade at $\Psi = 90^{\circ}$ ($V/\Omega R = 0.18$, untwisted blade)

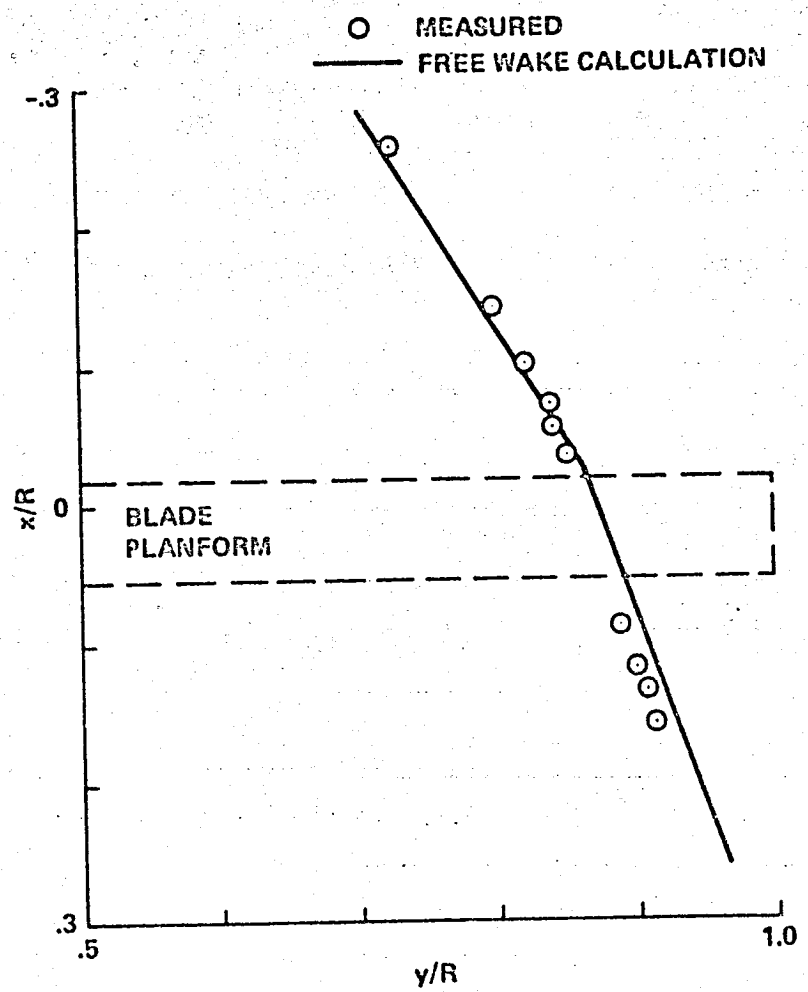

Figure 13. Top view of tip vortex geometry in vicinity of blade at $\Psi = 90^\circ$ ($V/\Omega R = 0.18$, -11° twist blade)

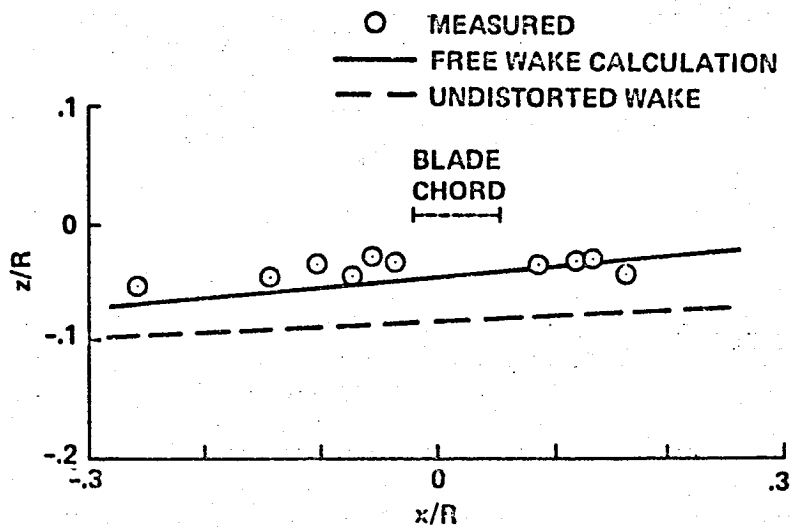

Figure 14. Side view of tip vortex geometry in vicinity of blade at $\psi = 90^{\circ}$ ($V/\Omega R = 0.18$, -11° twist blade)

END

DATE

FILMED

JUL 23 1980